RSC Advances

PAPER

View Article Online
View Journal | View Issue

Cite this: *RSC Adv.*, 2025, **15**, 24544

Photochemical [2 + 2] cycloadditions of naphthalene acrylic acids: templated and untemplated photoreactivity, selective homo/heterodimerizations, and conformational analysis†

Merve Temel, [a] Gizem Yildiz, [a] Kaan Berkay Ceyhan, [a] Fahri Alkan, [a] Onur Şahin [b] and Yunus E. Türkmen *[ac]

Received 26th May 2025
Accepted 7th July 2025

DOI: 10.1039/d5ra03698d

rsc.li/rsc-advances

Selective homo- and heterodimerization reactions of naphthalene acrylic acids have been achieved in a diastereocontrolled manner with the use of 1,8-dihydroxynaphthalene as a covalent template in photochemical [2 + 2] cycloadditions. When the reactions were run in solution, cycloaddition products were obtained in good yields (64–88%), which were subsequently detached from the template *via* a transesterification reaction affording the symmetrical and unsymmetrical cyclobutane products in 75–91% yields. A careful examination of the crystal structures of diester **6a** and cycloadduct **15a** along with detailed powder XRD and ATR-IR spectroscopic studies revealed an intriguing case of conformational isomerism in **15a** arising from the different possible orientations of its two ester carbonyls. The rotational barriers between the different conformers of **15a** were calculated to be within the range of 4.19–7.10 kcal mol^{-1}, indicative of rapid interconversion between these conformers in solution at room temperature.

Introduction

Photodimerization reactions of cinnamic acids and related analogues to access multisubstituted cyclobutanes comprise an important subclass of photochemical [2 + 2] cycloadditions of olefins.[1] Dimers of cinnamic acid derivatives, namely truxillic and truxinic acids, esters and amides, attracted significant attention from the synthetic community due to their presence in many cyclobutane-containing natural products, their interesting biological activities, and applications in polymer chemistry and materials science.[2] A variety of template-directed strategies[3] have been developed over the years in order to achieve [2 + 2] photodimerization of olefins in a regio- and stereoselective manner in both solid state[4] and solution phase.[5] In this respect, the use of diol- and bis-aniline-based covalent templates proved to be especially useful for the selective photochemical [2 + 2] cycloadditions of cinnamic acids.[6] Moreover, Benaglia and co-workers developed in 2023 a chiral auxiliary-based approach to access δ-truxinate products with high enantiomeric excess values.[7] Recently, in their elegant work, Yoon and co-workers reported enantioselective synthesis of β- and δ-truxinates as well as selective synthesis of α-truxillates.[8]

Despite these advances in the photodimerization reactions of cinnamic acid derivatives, photocycloadditions of acrylic acids substituted with polycyclic aromatic groups have been considerably less explored.[9] In one such study, Sawaki and co-workers reported in 1993 the photochemical [2 + 2] cycloaddition of sodium 1-naphthyl acrylate (**1**) in the presence of hydrotalcite clays, which gave the β-truxinate cycloadduct **2** in 75% yield along with the formation of *cis*-olefin **3** (25%, Scheme 1a).[9b] More recently, Mutlu, Barner-Kowollik and co-workers utilized the reversible [2 + 2] cycloaddition of 1-pyrenyl acrylic acid esters (**4**) giving cyclobutanes **5** in the design of systems that exhibit orthogonal photochemical reactivity in a single molecule (Scheme 1b).[9d] In 2020, Lu and co-workers investigated the photomechanical effects of [2 + 2] cycloaddition reactions of halogen-substituted 2-naphthalene acrylic acids, where the crystals of F–, Cl–, and Br-substituted 2-naphthalene acrylic acid derivatives were found to undergo a variety of motions such as bending, rotating, bursting, *etc.* upon irradiation with UV light.[9e] In 2021, we utilized 1,8-dihydroxynaphthalene (1,8-DHN) as a diol-based covalent template to provide a general solution to the selective homo- and heterodimerization of cinnamic acids (Scheme 1c).[10] Recently, we extended our

[a]*Department of Chemistry, Faculty of Science, Bilkent University, Ankara, 06800, Turkiye. E-mail: yeturkmen@bilkent.edu.tr*

[b]*Department of Occupational Health & Safety, Faculty of Health Sciences, Sinop University, Sinop 57000, Turkiye*

[c]*UNAM, National Nanotechnology Research Center, Institute of Materials Science and Nanotechnology, Bilkent University, Ankara, 06800, Turkiye*

† Electronic supplementary information (ESI) available. CCDC 2426760 and 2426761. For ESI and crystallographic data in CIF or other electronic format see DOI: https://doi.org/10.1039/d5ra03698d

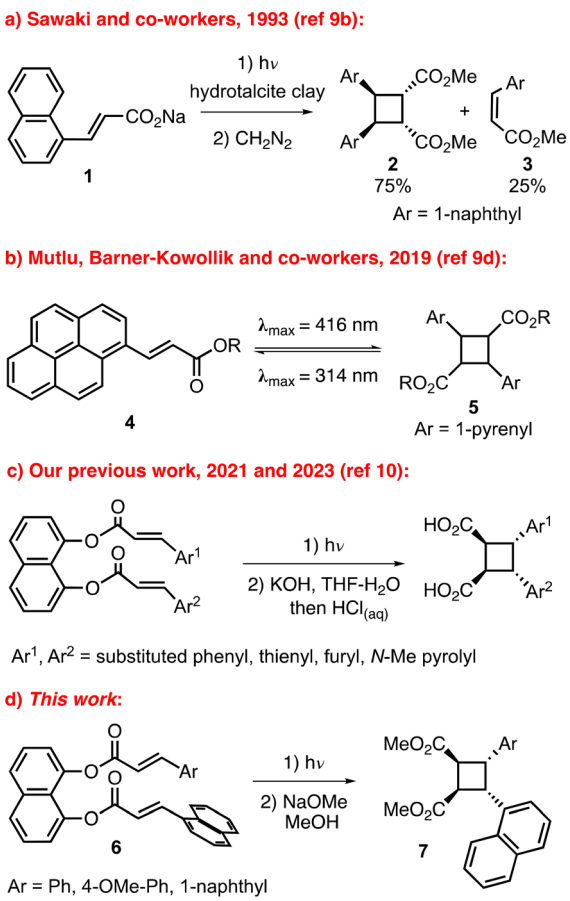

Scheme 1 Examples of photodimerization of β-aryl acrylic acids with aryl groups larger than a phenyl ring, and our work.

methodology to the photodimerization reactions of vinylogous cinnamic acids to access symmetrical and unsymmetrical dialkenyl cyclobutanes.[11] In the present work, we aimed to apply our template-directed strategy to the photodimerization of naphthalene acrylic acids (Scheme 1d).

There are a number of reasons for our interest in the photocycloadditions of this class of compounds. First, modification of a phenyl to a naphthyl ring, while seemingly simple, was shown to lead to superior results in various research areas possibly due to the larger size of the naphthyl ring in addition to its higher capability to participate in CH–π and π–π interactions compared to the phenyl ring. For instance, the presence of the naphthyl groups in 2-methoxy-2-naphthylpropanoic acids was shown by the Harada and Ichikawa groups to be highly beneficial in chiral recognition,[12] and determination of absolute configuration of alcohols.[13] Moreover, it was shown by Rawal and co-workers that much higher catalytic activity and enantioselectivity levels were obtained with the use of a 1-naphthyl-substituted taddol derivative as hydrogen bonding catalyst in enantioselective Diels–Alder reactions compared to the phenyl-substituted taddol catalyst.[14] Second, the higher conjugation of the π system present in naphthalene acrylic acids was expected to change their photophysical and photochemical properties,[15] which might affect their photoreactivity in [2 + 2] cycloadditions as well as their stabilities due to *cis–trans* isomerization under UV light or daylight. Finally, the larger size of the naphthyl ring has the potential to affect the crystal structures of template-bound naphthalene acrylic acids, which may lead to altered photochemical reactivity in solid state. Due to these reasons, we investigated in this work the photodimerization of naphthalene acrylic acids in solid state and in solution with the use of 1,8-DHN as a covalent template (Scheme 1d). In this regard, we achieved highly selective homo- and heterodimerizations of naphthalene acrylic acids, and compared the efficiencies and outcomes of the templated and untemplated photocycloadditions. Moreover, we performed a careful conformational analysis of the template-bound cycloadducts, which led to the identification of a highly interesting example of conformational isomerism. This phenomenon emerges as a result of the parallel and anti-parallel orientations of the C=O groups with respect to each other in the template-bound, photochemical [2 + 2] cycloaddition products. Such instances of conformational isomerism are attractive from a stereochemical viewpoint, as they have the potential to lead to atropisomerism depending on the energy barrier for the interconversion of the specific conformers.

Results and discussion

Photochemical [2 + 2] cycloadditions of template-bound naphthalene acrylic acids

Our studies commenced with the synthesis of the template-bound cycloaddition precursors **6a–c** (Scheme 2). For this purpose, we first prepared (*E*)-3-(naphthalen-1-yl)acrylic acid (**10**) in three steps starting from the commercially available 1-naphthol. Triflation of 1-naphthol with Tf_2O in the presence of Et_3N gave naphthyl triflate **8** in 95% yield. A subsequent Pd-catalyzed Heck coupling of **8** with methyl acrylate afforded α,β-unsaturated ester **9** in excellent yield (98%). The targeted 1-naphthalene acrylic acid **10** was obtained in 90% yield upon a final basic hydrolysis of ester **9**. The ^3J coupling constants of the olefinic protons of **9** and **10** were determined to be 15.8 and 15.7 Hz, respectively, which indicate that both compounds have *trans* alkene configurations.

With the naphthalene acrylic acid **10** in hand, we next synthesized the symmetrical diester **6a** *via* the esterification of 1,8-DHN (**12**) with **10** using DCC (*N*,*N*′-dicyclohexylcarbodiimide) and DMAP (4-dimethylaminopyridine) in 48% yield (Scheme 2). Preparation of the desired unsymmetrical cycloaddition precursors **6b** and **6c** required the sequential introduction of two different α,β-unsaturated acyl groups to 1,8-DHN. To this end, first the previously reported mono-ester **13**,[10a] was prepared by the mono-acylation of 1,8-DHN (**12**) with *trans*-cinnamoyl chloride in 78% yield. A second acylation of mono-ester **13** with the use of 1-naphthalene acryloyl chloride **11**, which in turn was prepared from **10** *via* its reaction with oxalyl chloride, and NaH as base afforded the unsymmetrical diester **6b** in 50% yield. A similar strategy was undertaken for the synthesis of diester **6c**. Initially, the known mono-ester **14**,[10a] was prepared in 76% yield from 1,8-DHN. The second acylation of mono-ester **14** with acyl chloride **11** in the presence of NaH

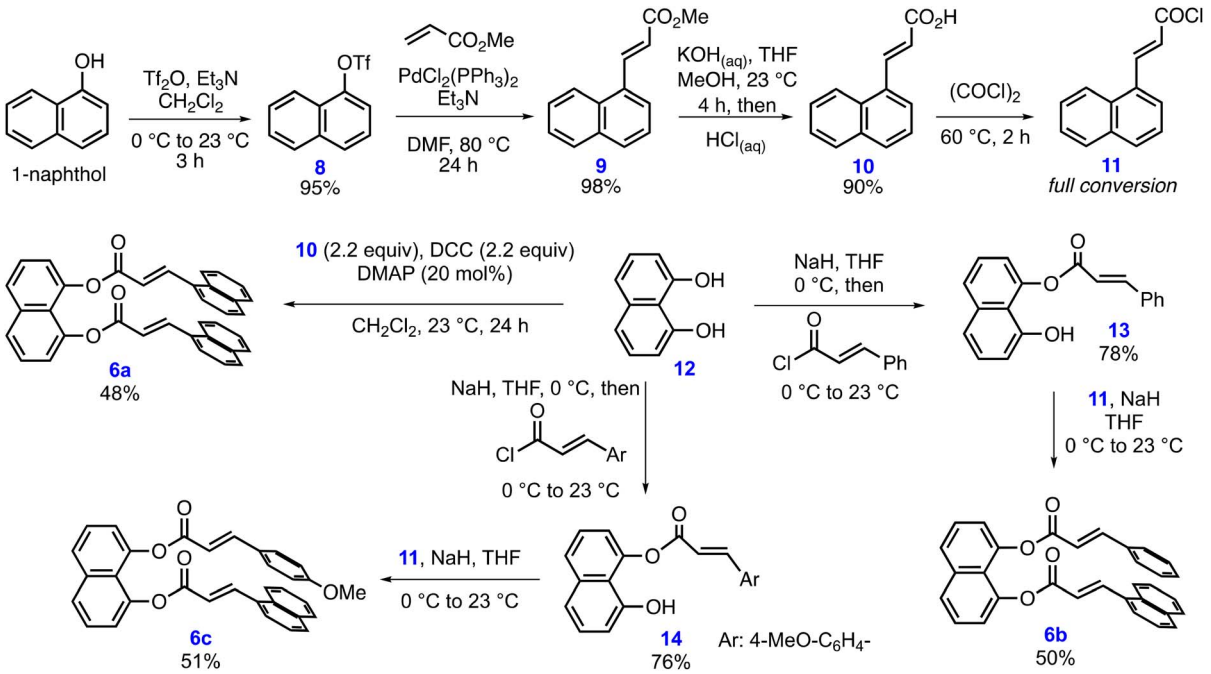

Scheme 2 Synthesis of the [2 + 2] cycloaddition precursors **6a–c**.

resulted in the formation of the unsymmetrical cycloaddition precursor **6c** in 51% yield.

Following the successful synthesis of the cycloaddition precursors **6**, we next investigated their [2 + 2] photodimerization reactions. To our delight, the irradiation of a powder sample of **6a** with UV-A light (365 nm, 4 × 9 W fluorescent lamps) afforded [2 + 2] cycloadduct **15a** in 88% yield as a single diastereomer (Table 1, entry 1). Moreover, the photochemical cycloaddition of the same compound in $CHCl_3$ solution was found to work equally well (88% yield, entry 1). Single crystals of diester **6a** were grown by the vapor diffusion of *n*-pentane to its solution in CH_2Cl_2. Single-crystal X-ray analysis of **6a** (CCDC 2426760) revealed an almost parallel orientation of the reacting olefins with a distance of 3.71 Å between their centroids (Fig. 1a and S1†), which is in accordance with the Schmidt criteria,[1c] and hence provides a rationale for the successful cycloaddition result that we obtained in solid state. The two naphthalene rings are also close to being parallel to each other with a dihedral angle of 4° between the two naphthalene planes. In addition, the shortest distance of the centroid of one of the phenyl rings of the top naphthalene to the plane formed by the bottom naphthalene in Fig. 1a was observed to be 3.54 Å, which is indicative of a strong π–π stacking interaction between the two naphthalene rings. Furthermore, the crystal structure of **6a** exhibited several intermolecular CH–π interactions with distances ranging between 2.74 and 2.94 Å (Fig. S2†).[16] The structure of cycloadduct **15a** was also analyzed by single-crystal X-ray crystallography (CCDC 2426761) confirming its β-truxinate nature and thus, the stereochemistry of the cycloaddition process (Fig. 1b, S3 and S4†). We should also add that we observed small amounts of product formation when compound **6a** was kept in solution under ambient laboratory conditions. In order to check this in a controlled manner, a solution of **6a** in $CDCl_3$ in an NMR tube was exposed to daylight, and the conversion of **6a** to **15a** was regularly checked by ^{1}H NMR spectroscopy (Fig. S5 and S6†). The conversion values were determined to be 25 and 38% after 48 and 72 h, respectively, whereas cycloadduct **15a** was observed to form with 96% conversion at the end of 15 days. These results show that for the template-bound diester **6a**, the major pathway in solution under daylight is the photochemical [2 + 2] cycloaddition without any significant *cis–trans* isomerization of the olefins.

With the successful results that we obtained on the homodimerization of **6a**, we turned our attention to the photochemical heterodimerization reactions of diesters **6b** and **6c** with the aim of constructing unsymmetrical β-truxinic acid analogues. Whereas the photochemical cycloaddition of diester **6b** worked poorly in solid state (11% yield), the heterodimerization product **15b** was isolated in 64% yield upon irradiation of **6b** in solution (Table 1, entry 2). Similarly, the heterodimerization of **6c** bearing the 1-naphthyl and 4-methoxyphenyl substituents proceeded smoothly in solution with an isolated product yield of 85% compared to 35% yield in solid state (entry 3). The inferior results obtained for the cycloaddition of diesters **6b** and **6c** in the solid state may be due to a less suitable geometric orientation of their reacting olefins in their solid-state structures. The cycloadducts **15a–c** were all detached from the template *via* a transesterification reaction using NaOMe in a 1 : 1 mixture of methanol and THF. At the end of these reactions, the cyclobutane dicarboxylic acid methyl esters **7a–c** were isolated in 75–91% yields as single diastereomers (Table 1, entries 1–3).

Table 1 Photochemical [2 + 2] cycloadditions of diesters **6** and synthesis of cyclobutane diesters **7**

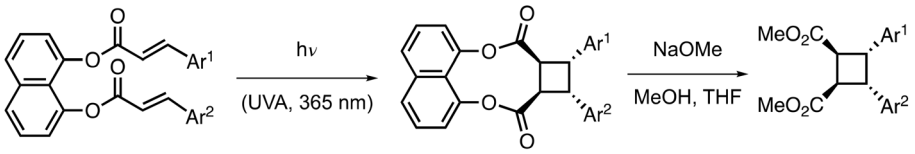

Ar^1 = 1-naphthyl (**6a**), Ph (**6b**), 4-OMe-Ph (**6c**)
Ar^2 = 1-naphthyl

Entry	Cycloaddition product	Yield of 15 (%)[a] Powder	solution[b]	Final product	Yield of 7 (%)[a]
1	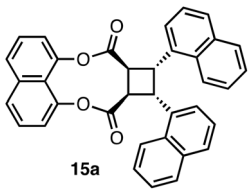 **15a**	88	88 (dr = 97 : 3)[c]	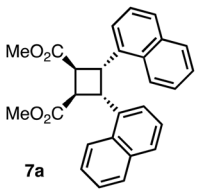 **7a**	75
2	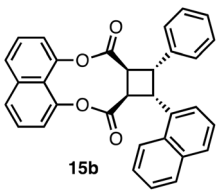 **15b**	11	64 (dr = 93 : 7)[c]	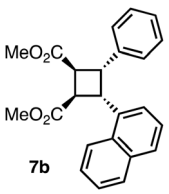 **7b**	91
3	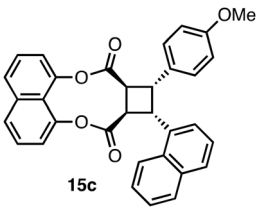 **15c**	35	85 (dr = 96 : 4)[c]	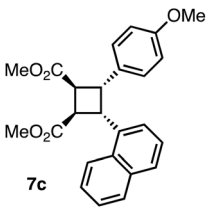 **7c**	87

[a] Yields refer to isolated product yields after purification by column chromatography. [b] Photochemical solution reactions were conducted in $CHCl_3$ in quartz test tubes. [c] Diastereomeric ratio (dr) values of the crude reaction mixtures were determined by ^{1}H NMR spectroscopy. The products were obtained as single diastereomers after purification.

Irradiation of crystals of diester 6a

Single-crystal-to-single-crystal (SCSC) transformations, where crystals retain their crystallinity at the end of chemical reactions, attracted considerable attention from the synthetic and crystallography communities.[17] Following the success of the cycloaddition of diester **6a** in powder form, we were curious to check if crystals of **6a** would undergo photochemical [2 + 2] cycloaddition in an SCSC manner. When we irradiated crystals of diester **6a** with UV light (365 nm), crystals did not crumble, and retained their integrity in terms of their shapes (Fig. 2 and S7†). We were also pleased to see that the cycloaddition reactions proceeded with full conversion within 20 h, as confirmed by ^{1}H-NMR spectroscopy (Fig. 3).

However, disappointingly, during the course of the irradiation, crystals were observed to turn orange from colourless, lose their transparency, and become opaque (Fig. 2 and S7†).‡ As a consequence, despite our extensive efforts, single-crystal X-ray analysis of the crystals after irradiation with UV light did not give any diffraction.

A closer look at the crystal structures of **6a** and **15a** revealed the possibility of an interesting conformational isomerism for cycloadduct **15a**, which arises from the different orientations of its carbonyl groups (Fig. 1 and Scheme 3). The three possible conformers of **15a** are shown in Scheme 3a, where the stereochemical descriptors *syn* and *anti* are used to indicate the relative relationship between the corresponding C=O group and the cyclobutane C–H, while the descriptor *cis* is used to describe the relative arrangement of the relevant C–H groups on the cyclobutane ring. It should be noted that the fourth possible conformation, namely the *syn-cis-anti* conformer, is the enantiomer of the already shown *anti-cis-syn* conformer, and therefore it was not included in Scheme 3a. In the X-ray structure of diester **6a**, the two carbonyls have an anti-parallel orientation, whereas its two olefins are almost parallel to each other (Fig. 1a). The [2 + 2] cycloaddition of crystals of **6a** is expected to

‡ The source of this orange color may be an oxidation process occurring on the surface of the crystals of **6a** during irradiation.

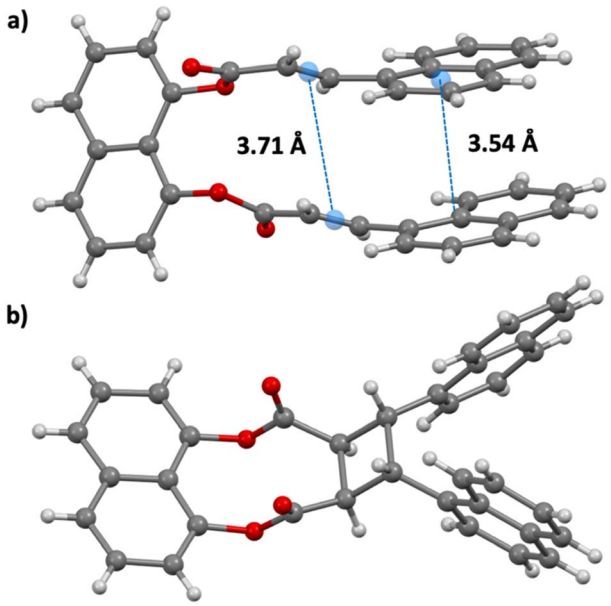

Fig. 1 X-ray crystal structures of (a) **6a**, and (b) **15a**.

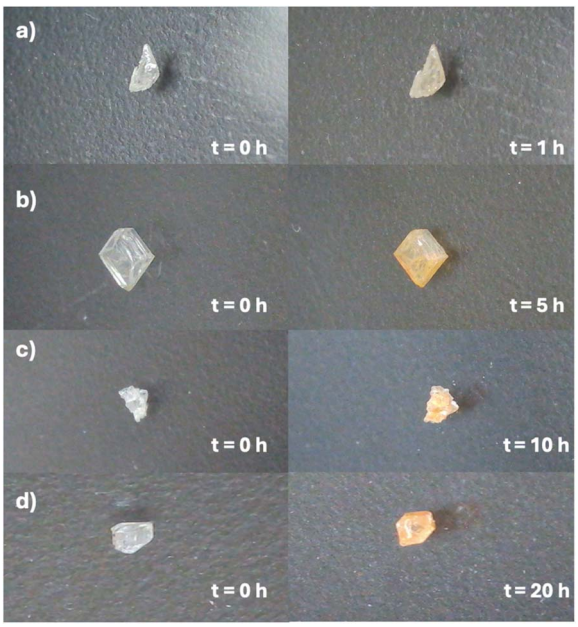

Fig. 2 Appearance of four crystals of **6a** after irradiation for (a) 1 h, (b) 5 h, (c) 10 h, and (d) 20 h.

proceed with retention of the orientations of the carbonyls affording the *anti-cis-syn* conformer of cycloadduct **15a** (**15a-1**, Scheme 3b). However, as explained in the previous section, when cycloadduct **15a** was purified by column chromatography and recrystallized, its X-ray analysis indicated the *anti-cis-anti* conformer (**15a-4**, Scheme 3b) with the C=O groups having a parallel orientation (Fig. 1b). In order to check if **15a-1** is different from **15a-4**, we performed a series of powder XRD and ATR-IR studies. Firstly, we wanted to confirm that the bulk structure of **15a-3** in powder form is the same as **15a-4**, which

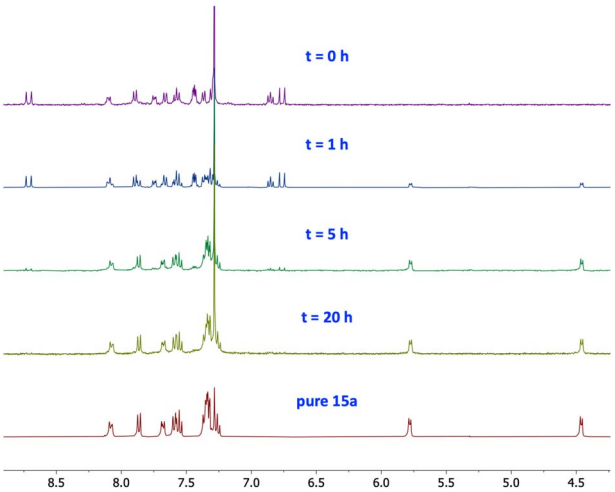

Fig. 3 Stacked ^{1}H-NMR spectra for the conversion of different crystals of diester **6a** to cycloadduct **15a** at different irradiation times.

was secured by X-ray crystallography. The powder XRD spectrum of **15a-3** is in nearly perfect agreement with the simulated powder XRD pattern of **15a-4** generated based on its single-crystal XRD data, indicating that they both have the same solid-state structure as the *anti-cis-anti* conformer (Fig. S8†). Next, we sought to compare the structures of **15a-2** and **15a-3**. To this end, **15a-1** crystals, which were obtained *via* the irradiation of the crystals of **6a**, were gently ground and analyzed by powder XRD. The powder XRD spectrum of **15a-2** showed differences compared to the spectrum of **15a-3**, supporting our hypothesis that **15a-2** and thus **15a-1** might be a conformational isomer of **15a-3** (Fig. S8† and Scheme 3b).

The proposed conformational isomerism of the different solid forms of the cycloadduct **15a** was further investigated by ATR-IR spectroscopy (Fig. 4 and S9–S12†). Whereas the ATR-IR spectrum of **15a-1** displays a strong C=O stretching band at 1760 cm^{-1}, the spectrum of **15a-3** surprisingly shows two separate signals in this region at 1740 and 1766 cm^{-1}, indicating a clear difference in the structures of these two solid forms of **15a** (Fig. 4, S10 and S11†). The reason for observing two C=O stretching bands for **15a-3** is not clear, but in its X-ray structure, the two carbonyl oxygens of **15a-4** participate in different CH–O interactions with varying CH···O distances (Fig. S4†).[18] These CH–O interactions with different strengths may cause the two carbonyls to display two separate IR bands. Finally, we should note that the ATR-IR spectra of **15a-3** and **15a-4** were found to be similar confirming that they are both *anti-cis-anti* conformers (Fig. S12†).

Overall, based on the above considerations, we propose that irradiation of crystals of **6a** with the two carbonyls having anti-parallel orientation affords **15a-1**, which is the *anti-cis-syn* conformer of cycloadduct **15a**. This conformation is proposed to be locked in the solid state, presumably due to the lack of free rotation of the carbonyl groups inside the crystals. However, when any sample of **15a** is dissolved in a solvent and concentrated, the resulting powder sample (**15a-3**) has *anti-cis-anti* conformation. The recrystallization of **15a-3** results in the

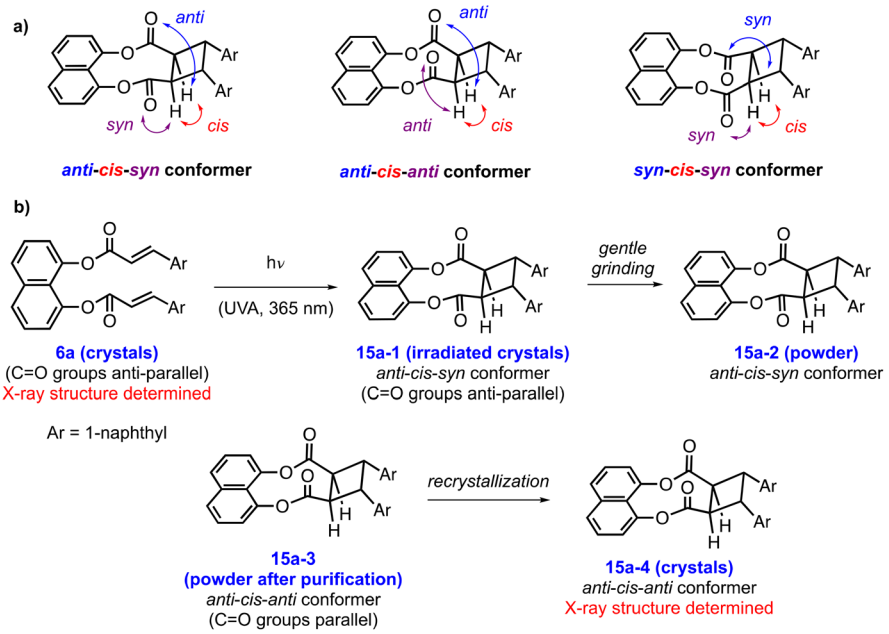

Scheme 3 (a) Stereochemical description of the possible conformers of cycloadduct **15a**; (b) different solid forms of **15a**, and their conformational relationships (Ar = 1-naphthyl).

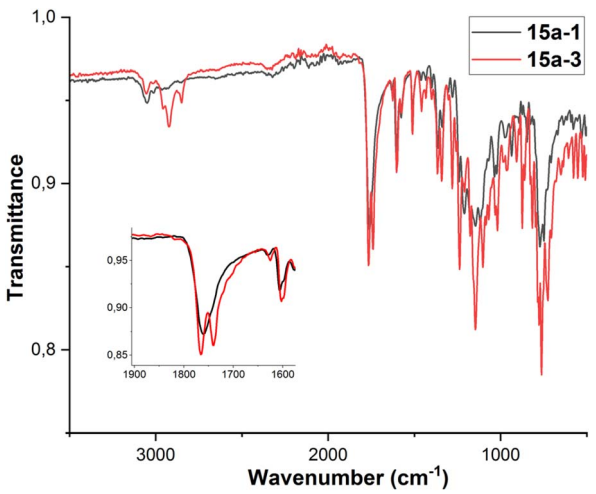

Fig. 4 Overlay of the ATR-IR spectra of **15a-1** and **15a-3**.

formation of **15a-4** crystals, which are also *anti-cis-anti* conformers of **15a** (Scheme 3). This may be due to the higher thermodynamic stability of the lattice structure of the *anti-cis-anti* conformer of **15a** compared to that of the *anti-cis-syn* conformer.

Computational investigation of the conformational isomers of 15a

Despite the differences mentioned above in the various solid forms of **15a** regarding their conformations, its ^{1}H and ^{13}C NMR spectra in $CDCl_3$ always displayed a single set of signals indicating either only one major conformation in solution or a rapid interconversion between different conformers. This prompted us to investigate computationally the energies of the different conformers of **15a** and the kinetic rotational barriers between these conformers.

The calculations were performed using the B3LYP functional,[19] with Grimmes D4 empirical dispersion corrections,[20] and Ahlrichs' def2-SVP basis set.[21] To minimize computational cost, the RIJCOSX approximation[22] was utilized alongside the def2/J auxiliary basis set[23] throughout the geometry optimizations of the initial and final states. The conductor-like polarizable continuum model (CPCM) was utilized to account for solvent effects using dichloromethane as the solvent in all computations.[24] This level of theory will be referred to as RIJCOSX-B3LYP-D4/def2-SVP as implemented in ORCA 6.0.1.[25] The minimum energy pathway (MEP) and the transition state between the different conformers were investigated with the nudged elastic band transition state (NEB-TS) procedure[26] as implemented in ORCA 6.0.1, employing 16 images between minima. All NEB-TS calculations and the optimization of the conformers of **15a** were carried out at the RIJCOSX-B3LYP-D4/def2-SVP level of theory. All calculated structures were generated and visualized using Gabedit[27] and Mercury[28] programs.

We first focused on the comparison of the **15a-*anti-cis-syn*** conformer, which corresponds to the solid-state **15a-1** structure in Scheme 3, and the **15a-*anti-cis-anti*** conformer, corresponding to the solid-state structure **15a-4** (Fig. 5). Please note that **15a-*anti-cis-syn*** conformer is chiral, whereas **15a-*anti-cis-anti*** conformer is achiral, increasing the importance of this analysis from a stereochemistry perspective. The energy difference between the **15a-*anti-cis-syn*** and **15a-*anti-cis-anti*** conformers was calculated to be 1.89 kcal mol^{-1}, with the *anti-cis-syn* conformer being more stable. Employing the NEB-TS method, the calculated activation barriers in both rotation directions

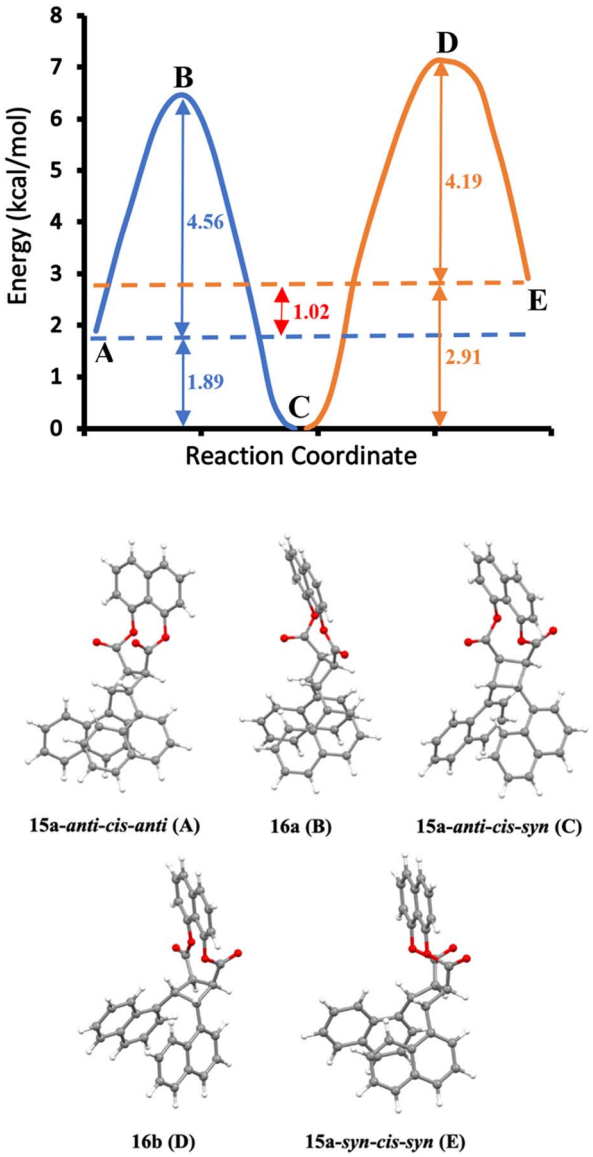

Fig. 5 The RIJCOSX-B3LYP-D4/def2-SVP reaction coordinates of 15a-*anti-cis-anti* (A) to 15a-*anti-cis-syn* (C) (blue), and 15a-*anti-cis-syn* (C) to 15a-*syn-cis-syn* (E) (orange). The relative energies of 15a-*anti-cis-anti* (A) is 1.89 kcal mol^{-1}, **16a** (B) is 6.45 kcal mol^{-1}, 15a-*anti-cis-syn* (C) is 0 kcal mol^{-1}, **16b** (D) is 7.10 kcal mol^{-1}, and 15a-*syn-cis-syn* (E) is 2.91 kcal mol^{-1}. The potential energy diagram was generated by employing 16 images between two minima (32 images in total) with NEB-TS formalism.

appeared to be 4.56 and 6.45 kcal mol^{-1}, both of which point to a facile, rapid interconversion between the two conformational isomers in solution at room temperature. It should also be noted that in the transition state structure of this rotation (**16a**), the planes of two carbonyl groups are almost perpendicular to each other with a dihedral angle of 86° (Fig. 5). Next, we considered the third possible conformer of **15a**, labeled as **15a-*syn-cis-syn*** in Fig. 5. This conformer was calculated to be slightly less stable than the **15a-*anti-cis-anti*** conformer being 1.02 kcal mol^{-1} higher in energy. The activation barriers for the interconversion between **15a-*anti-cis-syn*** and **15a-*syn-cis-syn*** were found to be 4.19 and 7.10 kcal mol^{-1} in the two rotation directions. This second transition state (**16b**) also has an almost perpendicular orientation of its two carbonyl groups. Overall, these computational studies indicate that the three conformational isomers of **15a** have close energies in solution (less than 3 kcal mol^{-1}) with activation barriers within the range of 4.19–7.10 kcal mol^{-1}. Therefore, it can be concluded that all three conformers of **15a** may coexist in solution with rapid interconversion at room temperature supporting its observed NMR spectroscopic features.

Photochemical reactivity of untemplated naphthalene acrylic acid derivatives

In the final stage of our studies, we examined the photochemical reactivities of the untemplated 1-naphthalene acrylic acid and ester derivatives. During our studies on the synthesis of the template-bound cycloaddition precursors, we observed that both naphthalene acrylic acid **10** and ester **9** were sensitive to daylight undergoing a *cis–trans* isomerization. In order to check this behaviour in a controlled manner, solutions of **9** ($E:Z$ = 98 : 2) in $CDCl_3$, and **10** (pure E isomer) in DMSO-d_6 were kept under ambient daylight for 11 days, and the *cis–trans* isomerization was analyzed regularly by ^{1}H-NMR spectroscopy. Whereas the formation of a [2 + 2] cycloadduct was not observed under these conditions, the $E:Z$ (*trans* : *cis*) ratio reached a constant value of 25 : 75 for ester **9**, and 15 : 85 for acid **10** after 9 days. The UV-vis absorption spectra of these compounds provide a rationale for their photochemical reactivities (Fig. S13 and S14†). The UV-vis spectrum of **9** (1×10^{-4} M in methanol) exhibited λ_{max} value at 323 nm with an absorption tail up to *ca.* 378 nm. Likewise, a solution of **10** (1×10^{-4} M in methanol) displays λ_{max} value at 322 nm in its UV-vis spectrum again with an absorption tail up to *ca.* 390 nm. The molar absorption coefficients (ε) of compounds **9** and **10** were determined to be 1.46×10^4 and 1.30×10^4 M^{-1} cm^{-1}, respectively, at their λ_{max} values. It should also be noted that the UV-vis spectrum of the cycloaddition precursor **6a** is very similar to those of **9** and **10** with a λ_{max} value of 326 nm ($\varepsilon = 3.04 \times 10^4$ M^{-1} cm^{-1}) and an absorption tail up to *ca.* 400 nm in CH_2Cl_2 (Fig. S15†). This provides a rationale for the observed photoreactivity of **6a** both with UV light at 365 nm and ambient daylight. Moreover, the diffuse reflectance UV-vis spectrum of **6a** recorded in solid powder form displayed absorbance below 398 nm (Fig. S16†). Finally, UV-vis absorption spectrum of cycloadduct **15a** revealed a λ_{max} value of 284 nm ($\varepsilon = 5.90 \times 10^3$ M^{-1} cm^{-1}) in CH_2Cl_2 (Fig. S17†). This decrease in the λ_{max} value for cycloadduct **15a** compared to compounds **6a**, **9** and **10**, which all have α,β-unsaturated ester and acid moieties, can be attributed to the reduced degree of conjugation in **15a** after cyclobutane ring formation.

Next, we investigated the irradiation of ester **9** in neat form as oil and in solution by UV-A light (Scheme 4a). The reaction of neat **9** afforded a mixture of β-truxinate **7a** and δ-truxinate **17** with 3 : 1 diastereomeric ratio (dr) and in 64% yield. The same reaction in a $CDCl_3$ solution proceeded without any diastereoselectivity, and a mixture of **7a** and **17** was observed to form in

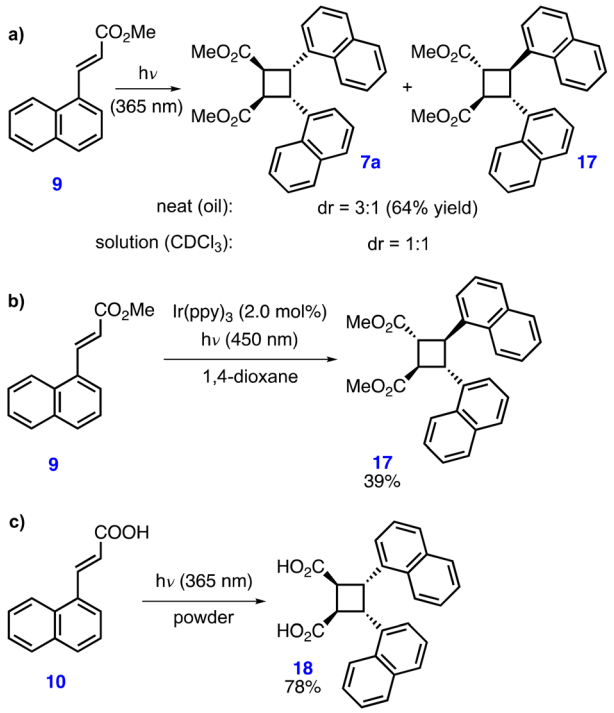

Scheme 4 Photochemical reactions of untemplated naphthalene acrylate **9** and acrylic acid **10**.

1 : 1 ratio. On the other hand, treatment of ester **9** with the $Ir(ppy)_3$ (tris(2-phenylpyridine)iridium) as a photocatalyst with visible light irradiation (450 nm) afforded δ-truxinate **17** as the major product with an unoptimized yield of 39% (Scheme 4b).[29] This result is not surprising as it was shown independently by the Wu and Reiser groups that visible-light catalysis of cinnamates proceeded *via* a [2 + 2] cycloaddition in an *anti*-head-to-head fashion giving δ-truxinic acid derivatives as the major products.[29,30] We then turned our attention to the photochemical behaviour of 1-naphthalene acrylic acid **10**. When a powder sample of **10** was irradiated with UV-A light (365 nm) for 20 h, β-truxinic acid product **18** was isolated in 78% yield (Scheme 4c). Despite all our attempts, we could not manage to get single crystals of compound **10** for X-ray analysis.

Conclusions

Our template-directed photochemical [2 + 2] cycloaddition strategy using 1,8-dihydroxynaphthalene as a covalent template has been employed for the selective homo- and hetero-dimerization of naphthalene acrylic acids. While the cycloaddition reactions work successfully both in solid state and solution, the reactions in solution were observed to give equal or higher yields (64–88%). After the final detachment of the template from cycloadducts, symmetrical and unsymmetrical β-truxinic acid dimethyl ester analogues bearing one or two naphthyl rings were isolated in good yields (75–91%). Single-crystal XRD analyses not only provided a geometrical rationale for the success of the cycloaddition of diester **6a** in solid state, but also confirmed the stereochemistry of the cycloadduct **15a**. Conformational isomers of **15a** in various solid forms, which are caused by the different possible orientations of the two carbonyl groups in powder and crystal forms, were carefully investigated by powder XRD and ATR-IR studies. Furthermore, computational analysis of the different conformers of **15a** revealed low barriers of rotation (up to 7.10 kcal mol^{-1}) in solution phase, which indicate fast interconversion between these conformational isomers of **15a** at room temperature. Finally, the untemplated photoreactivity of the naphthalene acrylic acid **10** and ester **9** was examined. Whereas the irradiation of ester **9** in neat oil form and in solution gave a mixture of the β and δ truxinate products, the δ truxinate product **17** and β truxinic acid product **18** could be obtained selectively, upon photocatalytic reaction of **9** and UV-A irradiation of **10**, respectively.

Experimental

General information

Air or water sensitive reactions were carried out under an inert atmosphere of nitrogen using oven-dried glassware. Reactions were monitored by thin-layer chromatography (TLC) using aluminium-backed plates pre-coated with silica gel (Silicycle, 60 Å, F_{254}). TLC visualization was done either by UV light (254 nm) or $KMnO_4$ staining solution. Silicycle 40–63 μm (200–400 mesh) silica gel was used for purification by flash column chromatography. NMR spectra were recorded using a Bruker spectrometer at 400 MHz for ^{1}H-NMR spectra and 100 MHz for ^{13}C $\{^1H\}$ spectra, and calibrated from internal standard (TMS, 0 ppm) or residual solvent signals (chloroform at 7.26, DMSO at 2.50, and acetone at 2.05 ppm for ^{1}H-NMR spectra; chloroform at 77.16, DMSO at 39.52, and acetone at 29.84 ppm for $^{13}C\{^1H\}$-NMR spectra). ^{1}H-NMR data are reported as follows: chemical shift (ppm, parts per million), integration, multiplicity (s = singlet, d = doublet, t = triplet, dd = doublet of doublets, m = multiplet, br s = broad signal, app = apparent), coupling constant (Hz). ATR-IR spectra were recorded using a Bruker Alpha-Platinum-ATR spectrometer, and selected peaks are reported. HRMS (high resolution mass spectrometry) analyses were conducted at UNAM-National Nanotechnology Research Center and Institute of Materials Science and Nanotechnology, Bilkent University, using Agilent Technologies 6224 TOF LC/MS instrument. Single-crystal XRD analysis was performed at the Scientific and Technological Research Application and Research Center, Sinop University, Türkiye. Powder XRD experiments were carried out using Malvern PANalytical (X'Pert PRO) X-ray diffractometer equipped with a Cu Kα X-ray source. An Agilent Cary 300 spectrophotometer was utilized for recording the UV-vis absorption spectra. Melting points are uncorrected. Photochemical reactions were conducted using a commercial UV gel nail dryer (Beurer, MP38) equipped with four 9W UV-A (365 nm) fluorescent lamps (Philips PL-S; Fig. S18†). Photographs of the crystals were acquired with a Ninyoon 4 K wifi digital microscope. Anhydrous CH_2Cl_2 and THF were purchased from Acros Organics (AcroSeal®). 1,8-dihydroxynaphthalene was purchased from abcr, and used as

received. All commercially available reagents were used without further purification, unless stated otherwise.

Naphthalen-1-yl trifluoromethanesulfonate (8)

This compound was prepared following the procedure reported in the literature.[31] An oven-dried, 100 mL round-bottomed flask was subjected to vacuum–nitrogen cycle three times, and then, 1-naphthol (500 mg, 3.47 mmol) was mixed with 5.0 mL of anhydrous CH_2Cl_2. When the solid dissolved completely, the reaction flask was inserted in an ice bath, and Et_3N (422 mg, 580 μL, 4.16 mmol) was added slowly. Afterwards, trifluoromethane sulfonic anhydride (1.08 g, 640 μL, 1.67 mmol) was added dropwise over 10 min. After *ca.* 10 min, the ice bath was removed, and the reaction mixture was stirred for 3 h at 23 °C. Then it was quenched with 5 mL of deionized water, and the aqueous phase was extracted three times with CH_2Cl_2. Anhydrous Na_2SO_4 was used to dry the combined organic phase. After the removal of the salt by filtration, the solvent was evaporated under reduced pressure. Purification by flash column chromatography (SiO_2; EtOAc : hexanes = 1 : 2) afforded compound **8** as a colourless oil (906 mg, 95% yield). ^{1}H NMR (400 MHz; $CDCl_3$) δ: 8.13 (1H, d, J = 8.3 Hz), 7.91 (1H, d, J = 8.0 Hz), 7.86 (1H, d, J = 6.8 Hz), 7.66 (1H, t, J = 7.6 Hz), 7.60 (1H, t, J = 7.5 Hz), 7.50–7.45 (2H, m). The ^{1}H NMR spectral data are in agreement with the data reported in the literature.[32]

Methyl (*E*)-3-(naphthalen-1-yl)acrylate (9)

An oven-dried, 25 mL Schlenk flask was subjected to vacuum–nitrogen cycle three times. Compound **8** (470 mg, 1.70 mmol) was dissolved in 10 mL of deoxygenated DMF, and methyl acrylate (732 mg, 792 μL, 8.50 mmol) was added to the reaction medium. Afterwards, Et_3N (860 mg, 1.18 mL, 8.50 mmol) and $PdCl_2(PPh_3)_2$ (59.6 mg, 0.085 mmol) were added sequentially. The Schlenk flask was then sealed with a glass stopper, and was heated gradually above the oil bath. After 10 min, it was dipped into a pre-heated oil bath at 80 °C. The reaction mixture was stirred at this temperature for 24 h. Then, the reaction mixture was cooled down to ambient temperature, and 5 mL of deionized water was added to quench the reaction. The mixture was transferred into a separatory funnel, and deionized water (5 mL) and brine (5 mL) were added. The product was extracted with EtOAc (3 × 10 mL). Anhydrous Na_2SO_4 was used to dry the combined organic phase. After the filtration of the salt, the solvent was evaporated under reduced pressure. Purification by column chromatography (SiO_2; EtOAc : hexanes = 1 : 9) afforded compound **9** as a colourless oil (354 mg, 98% yield). ^{1}H NMR (400 MHz; $CDCl_3$) δ: 8.55 (1H, d, J = 15.8 Hz), 8.20 (1H, d, J = 8.4 Hz), 7.88 (2H, app t, J = 7.0 Hz), 7.75 (1H, d, J = 7.2 Hz), 7.58 (1H, ddd, J = 8.5, 6.9 and 1.4 Hz), 7.53 (1H, ddd, J = 8.1, 6.8 and 1.4 Hz), 7.48 (1H, t, J = 7.7 Hz), 6.54 (1H, d, J = 15.7 Hz), 3.87 (3H, s). The ^{1}H NMR spectral data are in agreement with the data reported in the literature.[33]

(*E*)-3-(naphthalen-1-yl)acrylic acid (10)

In a 25 mL round-bottomed flask, compound **9** (77 mg, 0.36 mmol) was dissolved in 6 mL of a 1 : 2 mixture of MeOH : THF at 23 °C. An excess of 5 M aqueous solution of KOH (2.5 mL) was gradually added to the round-bottomed flask. After *ca.* 2 h, 0.5 mL additional KOH solution (5 M) was added. At the end of 4 h, TLC analysis indicated full consumption of the starting material. The reaction flask was placed in an ice bath, and HCl (*ca.* 1.2 M) was added into the flask to make the pH around 1–2. After the pH adjustment, the product was extracted by CH_2Cl_2 (3 × 10 mL). Anhydrous Na_2SO_4 was used to dry the combined organic phase. After the filtration of the salt, the solvent was evaporated under reduced pressure. Purification by flash column chromatography (SiO_2; 1% acetic acid in EtOAc : hexanes = 1 : 1) afforded compound **10** as a white solid (64.8 mg, 90% yield). M.P. 211.8–212.4 °C (lit. 210–213 °C).[34] ^{1}H NMR (400 MHz; DMSO-d_6) δ: 12.54 (1H, bs), 8.39 (1H, d, J = 15.7 Hz), 8.20 (1H, d, J = 8.3 Hz), 8.01 (2H, t, J = 9.0 Hz), 7.95 (1H, d, J = 7.1 Hz), 7.66–7.55 (3H, m), 6.60 (1H, d, J = 15.7 Hz). The ^{1}H NMR spectral data are in agreement with the data reported in the literature.[34]

Naphthalene-1,8-diyl (2*E*,2′*E*)-bis(3-(naphthalen-1-yl)acrylate) (6a)

An oven-dried, 25 mL round-bottomed flask was subjected to vacuum–nitrogen cycle three times. 1,8-DHN (**12**, 50.0 mg, 0.31 mmol) was dissolved in 4.0 mL of anhydrous CH_2Cl_2 under an inert atmosphere of N_2. Afterwards, compound **10** (136 mg, 0.68 mmol) was added to the flask. To completely dissolve compound **10**, additional 4.5 mL of anhydrous CH_2Cl_2 was added to the reaction medium. Sequentially, DCC (142 mg, 0.69 mmol) and DMAP (7.6 mg, 0.062 mmol) were added to the flask. The reaction mixture was stirred for 24 h under N_2 at 23 °C. It was then quenched with 10 mL of deionized water. The aqueous phase was extracted with CH_2Cl_2 (3 × 10 mL). The combined organic phase was dried over anhydrous Na_2SO_4. After the filtration of the salt, the solvent was evaporated under reduced pressure. Purification by flash column chromatography (SiO_2; hexanes: DCM = 1 : 1) afforded diester **6a** as a light yellow solid (77 mg, 48% yield). R_f = 0.23 (1 : 1 DCM: hexanes). M.P. 223.5–225.2 °C (CH_2Cl_2/pentane). ^{1}H NMR (400 MHz; $CDCl_3$) δ: 8.61 (2H, d, J = 15.8 Hz), 8.01–7.98 (2H, m), 7.79 (2H, d, J = 8.4 Hz), 7.65–7.63 (2H, m), 7.56 (2H, d, J = 8.2 Hz), 7.47 (2H, t, J = 7.9 Hz), 7.36–7.31 (4H, m), 7.26 (2H, d, J = 7.2 Hz), 7.19 (2H, d, J = 7.7 Hz), 6.75 (2H, t, J = 7.7 Hz), 6.66 (2H, d, J = 15.8 Hz). ^{13}C{^{1}H} NMR (100 MHz; $CDCl_3$) δ: 165.9, 145.5, 143.7, 137.0, 133.6, 131.3, 130.9, 130.7, 128.7, 127.1, 126.3, 126.2, 125.2, 125.0, 123.0, 121.6, 120.8, 119.6. FTIR ν_{max} (ATR, solid) per cm 3058, 1717, 1628, 1602, 1575, 1507, 1370, 1346. HRMS (APCI+) calcd for $C_{36}H_{25}O_4$ $[M + H]^+$: 521.1747, found: 521.1740.

Crystallization of compound 6a

In a 2.0 mL vial, 15.0 mg (0.029 mmol) of compound **6a** was dissolved in 1.0 mL of CH_2Cl_2. When the solution became clear, it was placed inside a 20 mL scintillation vial that contained *ca.* 7.5 mL of *n*-pentane. The lid of the outer vial was sealed with parafilm. To keep it under dark, it was stored inside a cabinet. Crystal formation was started to be observed within 24 h, and

crystals were collected after two additional days. Single crystals had transparent-white appearance.

8-(Cinnamoyloxy)naphthalen-1-yl (*E*)-3-(naphthalen-1-yl) acrylate (6b)

Initially, acyl chloride **11** was prepared by dissolving 1-naphthalene acrylic acid **10** (51.8 mg, 0.26 mmol) in 0.7 mL of oxalyl chloride under N_2 at 23 °C. After 10 min, the round-bottomed flask was inserted into a pre-heated oil bath at 60 °C, and was stirred for 2 h. At the end of this time, the reaction flask was cooled to ambient temperature, and the unreacted oxalyl chloride was evaporated carefully using a rotary evaporator. The resulting acyl chloride **11** (56.6 mg, 0.26 mmol) was obtained as a yellow solid. For the synthesis of diester **6b**, an oven-dried 50 mL round-bottomed flask was subjected to vacuum–nitrogen cycle three times. Compound **13**,[10a] (65.9 mg, 0.22 mmol) was dissolved in 3.0 mL of anhydrous THF. When the solution became clear after 10 min, an ice bath was placed under the round-bottomed flask. Then, a solution of acyl chloride **11** (56.6 mg, 0.26 mmol) in 3.0 mL of anydrous THF was added to the reaction mixture. Then, NaH (10.0 mg, 0.25 mmol, 60% dispersion in mineral oil) was added in small portions. After 5 min, the ice bath was removed, and the reaction mixture was stirred overnight. It was then quenched with 10 mL of saturated aqueous NH_4Cl solution. The aqueous phase was extracted with EtOAc (3 × 10 mL). Combined organic phase was dried by over anhydrous Na_2SO_4. After the filtration of the salt, the solvent was removed under reduced pressure. Purification by flash column chromatography (SiO_2; hexanes: CH_2Cl_2 : MeOH = 8 : 1 : 1 to 7 : 1 : 1) afforded diester **6b** as a yellow solid (53.9 mg, 50% yield). R_f = 0.21 (hexanes: CH_2Cl_2 : MeOH = 7 : 1 : 1). M.P. 147.8–148.8 °C. ^{1}H NMR (400 MHz; $CDCl_3$) δ: 8.72 (1H, d, J = 15.8 Hz), 8.17 (1H, d, J = 8.2 Hz), 7.82–7.78 (4H, m), 7.74 (1H, d, J = 8.2 Hz), 7.54–7.45 (5H, m), 7.24 (1H, d, J = 7.5 Hz), 7.21 (1H, d, J = 7.5 Hz), 7.14–7.10 (3H, m), 7.05 (1H, t, J = 7.7 Hz), 6.90 (2H, t, J = 7.7 Hz), 6.72 (1H, d, J = 15.8 Hz), 6.60 (1H, d, J = 16.0 Hz). ^{13}C{^{1}H} NMR (100 MHz; $CDCl_3$) δ: 166.0, 165.9, 147.1, 145.4, 143.6, 137.0, 133.8, 133.7, 131.5, 131.0, 130.9, 130.5, 128.8, 128.7, 128.0, 127.1, 127.0, 126.3, 126.2, 125.4, 125.1, 123.2, 121.5, 120.8, 119.6, 117.3. (26 signals were observed instead of the expected 30 signals in total, possibly due to the overlap of certain signals.) FTIR ν_{max} (ATR, solid) per cm 3059, 2925, 1729, 1633, 1604, 1574, 1432, 1366. HRMS (APCI+) calcd for $C_{32}H_{23}O_4$ $[M + H]^+$: 471.1591, found: 471.1596.

8-(((*E*)-3-(4-methoxyphenyl)acryloyl)oxy)naphthalen-1-yl (*E*)-3-(naphthalen-1-yl)acrylate (6c)

Initially, acyl chloride **11** was prepared by dissolving 1-naphthalene acrylic acid **10** (69.6 mg, 0.35 mmol) in 1.0 mL of oxalyl chloride under N_2 at 23 °C. After 10 min, the round-bottomed flask was dipped into pre-heated oil bath at 60 °C, and was stirred for 2 h. At the end of this time, the reaction flask was cooled to ambient temperature, and the unreacted oxalyl chloride was evaporated carefully using a rotary evaporator. The resulting acyl chloride **11** (76.1 mg, 0.35 mmol) was obtained as a yellow solid. However, 51.2 mg of compound **11** was used in the next step where diester **6c** was synthesized. An oven-dried 50 mL round-bottomed flask was subjected to vacuum–nitrogen cycle three times. Compound **14**,[10a] (52.7 mg, 0.216 mmol) was dissolved in 3.0 mL of anhydrous THF under nitrogen. When the solution became clear after 10 min, the flask was inserted into an ice bath. Then, acyl chloride **11** (51.2 mg, 0.23 mmol) was dissolved in 2.0 mL of anhydrous THF and was added to the reaction mixture. Then, NaH (6.5 mg, 0.164 mmol, 60% dispersion in mineral oil) was added in small portions. After 5 min, the ice bath was removed, and the reaction mixture was stirred overnight. It was then quenched with 10 mL of saturated aqueous solution of NH_4Cl. The aqueous phase was extracted with EtOAc (3 × 15 mL). The combined organic phase was dried by over anhydrous Na_2SO_4. After the filtration of the salt, the solvent was removed under reduced pressure. Purification by flash column chromatography (SiO_2; hexanes: CH_2Cl_2 : MeOH = 11 : 1 : 1 to 7 : 1 : 1) gave diester **6c** as a yellow solid (41.6 mg, 51% yield). R_f = 0.16 (hexanes: CH_2Cl_2 : MeOH = 7 : 1 : 1). M.P. 156.7–159.9 °C. ^{1}H NMR (400 MHz; $CDCl_3$) δ: 8.63 (1H, d, J = 15.8 Hz), 8.11 (1H, d, J = 8.1 Hz), 7.76–7.65 (5H, m), 7.49–7.41 (5H, m), 7.17 (1H, d, J = 7.3 Hz), 7.14 (1H, d, J = 7.5 Hz), 7.06 (1H, t, J = 7.7 Hz), 6.97 (2H, d, J = 8.7 Hz), 6.66 (1H, d, J = 15.8 Hz), 6.38 (1H, d, J = 15.9 Hz), 6.28 (2H, d, J = 8.6 Hz), 3.62 (3H, s). ^{13}C{^{1}H} NMR (100 MHz; $CDCl_3$) δ: 166.3, 165.9, 161.4, 146.8, 145.4, 143.3, 137.0, 133.8, 131.5, 131.0, 130.9, 129.7, 128.8, 127.1, 127.0, 126.9, 126.5, 126.3, 126.22, 126.17, 125.4, 125.23, 125.16, 123.2, 121.6, 120.8, 120.7, 119.8, 114.7, 114.0, 55.3. FTIR ν_{max} (ATR, solid) per cm 3061, 2933, 2911, 2835, 1714, 1629, 1601, 1573, 1510, 1463. HRMS (APCI+) calcd for $C_{33}H_{25}O_5$ $[M + H]^+$: 501.1697, found: 501.1693.

(8 a*R*,9*S*,10*R*,10 a*S*)-9,10-di(naphthalen-1-yl)-8a,9,10,10a-tetrahydrocyclobuta[*g*]naphtho [1,8-*bc*][1,5]dioxonine-8,11-dione (15a)

Irradiation in solution: diester **6a** (15.8 mg, 0.030 mmol) was dissolved in 3.5 mL of $CHCl_3$ in a quartz test tube. The tube was equipped with a stir bar, and placed inside the nail dryer (365 nm, 4 × 9 W fluorescent bulbs). A fan was used to control the temperature, and the reaction was monitored by TLC. At the end of 9 h, the solvent was removed under reduced pressure. Purification by flash column chromatography (SiO_2; DCM : hexanes = 1 : 2 to 1 : 1.2) afforded pure cycloadduct **15a** as a yellow solid (13.9 mg, 88% yield). Irradiation in solid state: diester **6a** (8.2 mg, 0.015 mmol) in powder form was placed between two quartz microscope slides. With the help of paper clips, the slides were fixed. They were then placed under UV lamps in a nail dryer (365 nm, 4 × 9 W). Every 4 h, the solid residue was mixed with a spatula. In addition to the mixing process to ensure homogeneous light distribution, the side of the slides facing the lamp was switched every 4 h. At the end of 16 h of irradiation, the conversion was determined as 98% by ^{1}H NMR analysis. Purification by flash column chromatography (SiO_2; DCM : hexanes = 1 : 1) afforded cycloadduct **15a** as a yellow solid (7.2 mg, 88% yield). R_f = 0.62 (1 : 1 DCM: hexanes). ^{1}H NMR (400 MHz; $CDCl_3$) δ: 7.99–7.96 (2H, m), 7.75 (2H, d, J = 7.9 Hz), 7.58–7.55 (2H, m), 7.48 (2H, d, J = 8.2 Hz),

7.44 (2H, t, $J = 8.0$ Hz),7.26–7.19 (8H, m), 7.17–7.13 (2H, m), 5.68 (2H, app d, $J = 6.2$ Hz), 4.35 (2H, app d, $J = 6.1$ Hz). $^{13}C\{^1H\}$ NMR (100 MHz; $CDCl_3$) δ: 170.0, 145.6, 137.2, 134.5, 133.6, 131.7, 128.7, 127.7, 127.1, 126.5, 126.0, 125.7, 124.9, 123.8, 123.7, 121.2, 119.8, 45.4, 41.1. FTIR ν_{max} (ATR, solid, **15a-3**) per cm 3052, 2958, 2922, 2851, 1766, 1740, 1603, 1512. FTIR ν_{max} (ATR, solid, **15a-1**) per cm 3050, 1760, 1606, 1577, 1510. HRMS (APCI+) calcd for $C_{36}H_{25}O_4$ $[M + H]^+$: 521.1747, found 521.1748.

Crystallization of compound 15a

In a 2.0 mL vial, 6.8 mg (0.013 mmol) of compound **15a** was dissolved in 1.0 mL of CH_2Cl_2. When the solution became clear, it was placed inside a 20 mL scintillation vial that contained *ca.* 7.5 mL of *n*-pentane. The lid of the outer vial was sealed with parafilm. To keep it under dark, it was stored inside a cabinet. Crystal formation was started to be observed within 24 h, and crystals were collected after two additional days. Single crystals had needle-like, yellowish-white appearance.

(8 a*R*,9*S*,10*R*,10 a*S*)-9-(naphthalen-1-yl)-10-phenyl-8a,9,10,10a-tetrahydrocyclobuta[*g*] naphtho[1,8-*bc*][1,5]dioxonine-8,11-dione (*rac*-15b)

Diester **6b** (23.6 mg, 0.050 mmol) was dissolved in 2.0 mL of $CHCl_3$ in a quartz test tube. The tube was equipped with a stir bar, and placed inside the nail dryer (365 nm, 4 × 9 W fluorescent bulbs). A fan was used to control the temperature, and the reaction was monitored by TLC. At the end of 20 h, the solvent was removed under reduced pressure. Purification by flash column chromatography (SiO_2; EtOAc : hexanes = 1 : 10 to 1 : 9) afforded cycloadduct **15b** as an amorphous foam (15.1 mg, 64% yield). $R_f = 0.42$ (hexanes: DCM : MeOH = 7 : 1 : 1). ^1H NMR (400 MHz; $CDCl_3$) δ: 7.98 (1H, d, $J = 8.4$ Hz), 7.82 (1H, dd, $J = 8.3$, 0.8 Hz), 7.81 (1H, dd, $J = 8.3$, 0.7 Hz), 7.71 (1H, d, $J = 7.8$ Hz), 7.62 (1H, dd, $J = 7.5$, 1.5 Hz), 7.55–7.44 (3H, m), 7.41–7.30 (4H, m), 7.25–7.23 (1H, m), 7.00–6.97 (2H, m), 6.95–6.90 (3H, m), 5.50 (1H, t, $J = 9.5$ Hz), 4.87 (1H, dd, $J = 10.2$, 4.9 Hz), 4.66 (1H, t, $J = 9.8$ Hz), 4.16 (1H, ddd, $J = 10.8$, 4.8, 1.1 Hz). $^{13}C\{^1H\}$ NMR (100 MHz; $CDCl_3$) δ: 170.4, 169.7, 145.54, 145.49, 138.1, 137.1, 133.7, 133.6, 131.5, 128.7, 128.0, 127.7, 127.10, 127.09, 126.9, 126.6, 126.0, 125.9, 125.0, 124.1, 123.9, 121.2, 121.1, 119.7, 45.3, 43.8, 42.2. (27 signals were observed instead of the expected 30 signals in total, possibly due to the overlap of certain signals.) FTIR ν_{max} (ATR, solid) per cm 2959, 2922, 2852, 1762, 1607, 1455, 1365. HRMS (APCI+) calcd for $C_{32}H_{23}O_4$ $[M + H]^+$: 471.1591, found: 471.1596.

(8 a*S*,9*R*,10*S*,10 a*R*)-9-(4-methoxyphenyl)-10-(naphthalen-1-yl)-8a,9,10,10a-tetrahydrocyclo buta[*g*]naphtho[1,8-*bc*][1,5] dioxonine-8,11-dione (*rac*-15c)

Diester **6c** (14.9 mg, 0.030 mmol) was dissolved in 2.0 mL of $CHCl_3$ in a quartz test tube. The tube was equipped with a stir bar, and placed inside the nail dryer (365 nm, 4 × 9 W fluorescent bulbs). A fan was used to control the temperature, and the reaction was monitored by TLC. At the end of 9 h, the solvent was removed under reduced pressure. Purification by flash column chromatography (SiO_2; EtOAc : hexanes = 1 : 10 to 1 : 7) afforded cycloadduct **15c** as yellowish-orange oil (12.6 mg, 85% yield). $R_f = 0.34$ (1 : 2 EtOAc : hexanes). ^1H NMR (400 MHz; $CDCl_3$) δ: 7.90 (1H, d, $J = 8.4$ Hz), 7.75 (1H, d, $J = 8.3$ Hz), 7.74 (1H, d, $J = 8.3$ Hz), 7.66 (1H, d, $J = 8.0$ Hz), 7.57 (1H, dd, $J = 6.9$, 2.1 Hz), 7.49–7.29 (6H, m), 7.24 (1H, d, $J = 7.5$ Hz), 7.17 (1H, d, $J = 8.4$ Hz), 6.84 (2H, d, $J = 8.6$ Hz), 6.40 (2H, d, $J = 8.6$ Hz), 5.40 (1H, t, $J = 9.4$ Hz), 4.76 (1H, dd, $J = 10.1$, 4.9 Hz), 4.58 (1H, t, $J = 9.8$ Hz), 4.04 (1H, dd, $J = 10.6$, 4.9 Hz), 3.51 (3H, s). $^{13}C\{^1H\}$ NMR (100 MHz; $CDCl_3$) δ: 170.5, 169.8, 158.3, 145.54, 145.48, 137.1, 133.9, 133.7, 131.5, 130.3, 129.0, 128.7, 127.7, 127.1, 126.5, 126.0, 125.9, 125.1, 124.2, 123.8, 121.2, 121.1, 119.7, 113.4, 55.2, 45.8, 44.7, 43.6, 42.4. (29 signals were observed instead of the expected 31 signals in total, possibly due to the overlap of certain signals.) FTIR ν_{max} (ATR, film) per cm 3058, 2954, 2922, 2850, 1760, 1732, 1629, 1607, 1577, 1513, 1364. HRMS (APCI+) calcd for $C_{33}H_{25}O_5$ $[M + H]^+$: 501.1697, found: 501.1699.

Dimethyl (1*R*,2*S*,3*R*,4*S*)-3,4-di(naphthalen-1-yl)cyclobutane-1,2-dicarboxylate (7a)

In a 20 mL scintillation vial, compound **15a** (18.2 mg, 0.035 mmol) was dissolved in 6.0 mL of 1 : 1 MeOH : THF mixture. To this clear solution, NaOMe (4.7 mg, 0.087 mmol) was then added. The resulting cloudy mixture was stirred at 23 °C for 8 h. At the end of this time, all volatiles were removed under reduced pressure. Purification by flash column chromatography (SiO_2; 1 : 1 = hexanes:CH_2Cl_2) afforded cyclobutane **7a** as a pale yellow solid (11.2 mg, 75% yield). $R_f = 0.39$ (1 : 1 hexanes:CH_2Cl_2). M.P. 182.3–184.2 °C. ^1H NMR (400 MHz; $CDCl_3$) δ: 7.90 (2H, d, $J = 8.2$ Hz), 7.51 (2H, d, $J = 8.4$ Hz), 7.40 (2H, dd, $J = 7.2$, 2.0 Hz), 7.20–7.13 (4H, m), 7.10–7.05 (4H, m), 5.32 (2H, app d, $J = 6.6$ Hz), 4.00 (2H, app d, $J = 6.3$ Hz), 3.72 (6H, s). $^{13}C\{^1H\}$ NMR (100 MHz; $CDCl_3$) δ: 173.1, 134.7, 133.5, 131.9, 128.5, 127.4, 125.7, 125.5, 124.8, 123.8, 123.6, 52.4, 43.9, 41.6. FTIR ν_{max} (ATR, solid) per cm 2951, 2919, 1720, 1596, 1510, 1430, 1363. HRMS (APCI+) calcd for $C_{28}H_{25}O_4$ $[M + H]^+$: 425.1747, found: 425.1745.

Dimethyl (1*S*,2*R*,3*S*,4*R*)-3-(naphthalen-1-yl)-4-phenylcyclobutane-1,2-dicarboxylate (*rac*-7b)

Compound **15b** (11.9 mg, 0.025 mmol) was dissolved in 3.0 mL of a 1 : 1 MeOH : THF mixture in a 20 mL scintillation vial. To this clear solution, NaOMe (6.8 mg, 0.13 mmol) was then added. The resulting mixture was stirred at 45 °C for 3.5 h. At the end of this time, all volatiles were removed under reduced pressure. Purification by flash column chromatography (SiO_2; EtOAc : hexanes = 1 : 11 to 1 : 5) afforded cyclobutane **7b** as orange oil (8.6 mg, 91% yield). $R_f = 0.30$ (1 : 5 EtOAc : hexanes). ^1H NMR (400 MHz; $CDCl_3$) δ: 7.96 (1H, d, $J = 8.4$ Hz), 7.69 (1H, d, $J = 8.0$ Hz), 7.57 (1H, d, $J = 8.2$ Hz), 7.45 (1H, t, $J = 7.6$ Hz), 7.38 (1H, t, $J = 7.4$ Hz), 7.29–7.26 (1H, m), 7.18 (1H, d, $J = 7.0$ Hz), 6.87 (5H, app s), 5.22 (1H, t, $J = 9.6$ Hz), 4.46 (1H, dd, $J = 9.9$, 4.7 Hz), 4.28 (1H, t, $J = 9.7$ Hz), 3.81 (3H, s), 3.80–3.76 (1H, m), 3.75 (3H, s). $^{13}C\{^1H\}$ NMR (100 MHz; $CDCl_3$) δ: 173.5, 172.8, 138.4, 134.3, 133.5, 131.7, 128.6, 127.8 (overlapping of two signals), 127.4, 126.6, 125.8, 125.7, 125.0, 124.2, 123.6, 52.5, 52.3, 46.1, 44.5, 42.7, 41.7. FTIR ν_{max} (ATR, film) per cm 2951, 2922, 2850, 1730,

1599, 1435. HRMS (APCI+) calcd for $C_{24}H_{23}O_4$ $[M + H]^+$: 375.1591, found: 375.1592.

Dimethyl (1*R*,2*S*,3*R*,4*S*)-3-(4-methoxyphenyl)-4-(naphthalen-1-yl)cyclobutane-1,2-dicarboxylate (*rac*-7c)

Compound **15c** (11.7 mg, 0.023 mmol) was dissolved in 3.0 mL of a 1 : 1 MeOH : THF mixture in a 20 mL scintillation vial. To this clear solution, NaOMe (6.3 mg, 0.12 mmol) was then added. The resulting mixture was stirred at 45 °C for 5 h. Purification by flash column chromatography (SiO_2; 1.25 : 1 = hexanes : EtOAc) afforded cyclobutane **7c** as yellowish oil (8.2 mg, 87% yield). R_f = 0.22 (1 : 5 EtOAc : hexanes). ^{1}H NMR (400 MHz; $CDCl_3$) δ: 7.93 (1H, d, J = 8.4 Hz), 7.70 (1H, d, J = 8.1 Hz), 7.58 (1H, d, J = 8.2 Hz), 7.44 (1H, t, J = 7.1 Hz), 7.38 (1H, t, J = 7.3 Hz), 7.29 (1H, t, J = 7.7 Hz), 7.19 (1H, d, J = 7.1 Hz), 6.78 (2H, d, J = 8.6 Hz), 6.41 (2H, d, J = 8.6 Hz), 5.17 (1H, t, J = 9.7 Hz), 4.41 (1H, dd, J = 9.9, 4.7 Hz), 4.26 (1H, t, J = 9.7 Hz), 3.80 (3H, s), 3.74 (3H, s), 3.71 (1H, dd, J = 10.2, 4.8 Hz), 3.56 (3H, s). ^{13}C{^{1}H} NMR (100 MHz; $CDCl_3$) δ: 173.5, 172.8, 158.1, 134.5, 133.6, 131.7, 130.7, 128.8, 128.6, 127.4, 125.8, 125.6, 125.0, 124.2, 123.5, 113.3, 55.1, 52.4, 52.3, 45.4, 45.0, 42.9, 41.6. FTIR ν_{max} (ATR, film) per cm 2951, 2924, 2850, 1727, 1610, 1513, 1435. HRMS (APCI+) calcd for $C_{25}H_{25}O_5$ $[M + H]^+$: 405.1697, found: 405.1693.

Dimethyl (1*R*,2*R*,3*S*,4*S*)-3,4-di(naphthalen-1-yl)cyclobutane-1,2-dicarboxylate (*rac*-17)

In this reaction, the procedure developed by Wu and co-workers has been applied.[29] In a quartz test tube, compound **9** (20.1 mg, 0.094 mmol) was dissolved in 0.94 mL of anhydrous 1,4-dioxane under nitrogen. Afterwards, tris(2-phenylpyridine)iridium(III) ($Ir(ppy)_3$, 1.2 mg, 0.0018 mmol) was added. The test tube was irradiated using 450 nm light for 8 h. At the end of this time, all volatiles were removed under reduced pressure. The ^{1}H NMR spectrum of the crude mixture indicated that the ratio of β truxinate isomer **7a** to the δ truxinate isomer **17** was 0.16 : 1.00. Purification by flash column chromatography (SiO_2; EtOAc : hexanes = 1 : 8 to 1 : 7) afforded cyclobutane **17** as a yellowish-white solid (7.9 mg, 39% yield). R_f = 0.32 (1 : 5 EtOAc : hexanes). M.P. 197.9–199.0 °C. ^{1}H NMR (400 MHz; $CDCl_3$) δ: 7.79 (2H, d, J = 8.2 Hz), 7.77–7.73 (6H, m), 7.50 (2H, t, J = 7.7 Hz), 7.36 (2H, ddd, J = 8.0, 6.8, 1.1 Hz), 7.21 (2H, ddd, J = 8.5, 6.8, 1.4 Hz), 4.75 (2H, app d, J = 9.5 Hz), 3.73 (2H, app d, J = 9.6 Hz), 3.71 (6H, s). ^{13}C{^{1}H} NMR (100 MHz; $CDCl_3$) δ: 173.4, 136.7, 133.9, 132.0, 128.7, 128.0, 126.0, 125.8, 125.7, 124.1, 123.6, 52.4, 45.3, 43.9. FTIR ν_{max} (ATR, solid) per cm 3050, 2954, 2923, 2850, 1723, 1597, 1510, 1445, 1435, 1397. HRMS (APCI+) calcd for $C_{28}H_{25}O_4$ $[M + H]^+$: 425.1747, found: 425.1742.

(1*R*,2*S*,3*R*,4*S*)-3,4-di(naphthalen-1-yl)cyclobutane-1,2-dicarboxylic acid (18)

Compound **10** (20.4 mg, 0.10 mmol) was placed between two quartz microscope slides. The slides were fixed with the help of paper clips. The solid was then irradiated by 365 nm UV light (4 × 9 W) using the nail dryer. Every 4 h, solid residue was mixed with a spatula. In addition to the mixing process to ensure homogenous light distribution, the side of the slides facing the lamp was turned every 4 h. The irradiation was continued for 20 h. Purification by flash column chromatography (SiO_2; 1% acetic acid in EtOAc) afforded cyclobutane **18** as a white solid (15.9 mg, 78% yield). R_f = 0.64 (1% acetic acid in EtOAc). M.P. 195 °C (decomp). ^{1}H NMR 400 MHz; (acetone-d_6) δ: 8.17 (2H, d, J = 7.7 Hz), 7.64–7.61 (2H, m), 7.52 (2H, d, J = 8.1 Hz), 7.46 (2H, d, J = 7.2 Hz), 7.30–7.21 (6H, m), 5.45–5.44 (2H, m), 4.22–4.21 (2H, m). ^{13}C{^{1}H} NMR (100 MHz; (acetone-d_6) δ: 174.1, 136.2, 134.4, 132.8, 129.2, 127.8, 126.3, 126.1, 125.7, 125.0, 124.7, 44.4, 42.2. FTIR ν_{max} (ATR, solid) per cm 3041, 2956, 2921, 2851, 1698, 1597, 1509, 1417, 1397. HRMS (APCI-) calcd for $C_{26}H_{19}O_4$ $[M–H]^-$: 395.1289, found: 395.1290.

Data availability

The data supporting this article have been included as part of the ESI.†

Conflicts of interest

There are no conflicts to declare.

Acknowledgements

The numerical calculations reported in this article were fully performed at TUBITAK ULAKBIM, High Performance and Grid Computing Center (TRUBA resources). Y. E. T. acknowledges financial support by the GEBIP Award of the Turkish Academy of Sciences. The authors also acknowledge the Scientific and Technological Research Application and Research Center, Sinop University, Türkiye, for the use of the Bruker D8 Quest diffractometer.

References

1 (*a*) S. Poplata, A. Tröster, Y.-Q. Zou and T. Bach, *Chem. Rev.*, 2016, **116**, 9748; (*b*) D. M. Bassani, The Dimerization of Cinnamic Acid Derivatives, in *CRC Handbook of Photochemistry and Photobiology*, ed. W. M. Horspool and F. Lenci, 2nd edn, CRC Press, Boca Raton, 2004; p. p. 20; (*c*) G. M. J. Schmidt, *Pure Appl. Chem.*, 1971, **27**, 647.

2 (*a*) P. Yang, Q. Jia, S. Song and X. Huang, *Nat. Prod. Rep.*, 2023, **40**, 1094; (*b*) X. Yuan, L. Men, Y. Liu, Y. Qiu, C. He and W. Huang, *J. Holistic Integr. Pharm.*, 2020, **1**, 48; (*c*) S. El-Arid, J. M. Lenihan, A. B. Beeler and M. W. Grinstaff, *Polym. Chem.*, 2024, **15**, 3935.

3 Selected examples:(*a*) L. R. MacGillivray, J. L. Reid and J. A. Ripmeester, *J. Am. Chem. Soc.*, 2000, **122**, 7817; (*b*) D. M. Bassani, V. Darcos, S. Mahony and J.-P. Desvergne, *J. Am. Chem. Soc.*, 2000, **122**, 8795; (*c*) G. S. Papaefstathiou, A. J. Kipp and L. R. MacGillivray, *Chem. Commun.*, 2001, 2462; (*d*) T. Caronna, R. Liantonio, T. A. Logothetis, P. Metrangolo, T. Pilati and G. Resnati, *J. Am. Chem. Soc.*, 2004, **126**, 4500; (*e*) X. Mei, S. Liu and C. Wolf, *Org. Lett.*, 2007, **9**, 2729; (*f*) B. R. Bhogala, B. Captain, A. Parthasarathy and V. Ramamurthy, *J. Am. Chem. Soc.*, 2010, **132**, 13434; (*g*) T. P. Martyanov, A. P. Vorozhtsov,

N. A. Aleksandrova, I. V. Sulimenkov, E. N. Ushakov and S. P. Gromov, *ACS Omega*, 2022, **7**, 42370; (*h*) J. Alfuth, O. Jeannin and M. Fourmigué, *Angew. Chem., Int. Ed.*, 2022, **61**, e202206249.

4 (*a*) L. R. MacGillivray, *J. Org. Chem.*, 2008, **73**, 3311; (*b*) L. R. MacGillivray, G. S. Papaefstathiou, T. Friščić, T. D. Hamilton, D.-K. Bučar, Q. Chu, D. B. Varshney and I. G. Georgiev, *Acc. Chem. Res.*, 2008, **41**, 280; (*c*) M. Nagarathinam, A. M. P. Peedikakkal and J. J. Vittal, *Chem. Commun.*, 2008, 5277; (*d*) K. Biradha and R. Santra, *Chem. Soc. Rev.*, 2013, **42**, 950; (*e*) M.-M. Gan, J.-G. Yu, Y.-Y. Wang and Y.-F. Han, *Cryst. Growth Des.*, 2018, **18**, 553.

5 (*a*) J. Svoboda and B. König, *Chem. Rev.*, 2006, **106**, 5413; (*b*) B. Bibal, C. Mongin and D. M. Bassani, *Chem. Soc. Rev.*, 2014, **43**, 4179.

6 (*a*) D. Haag and H.-D. Scharf, *J. Org. Chem.*, 1996, **61**, 6127; (*b*) B. König, S. Leue, C. Horn, A. Caudan, J.-P. Desvergne and H. Bouas-Laurent, *Liebigs Ann.*, 1996, 1231; (*c*) H. Zitt, I. Dix, H. Hopf and P. G. Jones, *Eur. J. Org Chem.*, 2002, 2298; (*d*) H. Yuasa, M. Nakatani and H. Hashimoto, *Org. Biomol. Chem.*, 2006, **4**, 3694; (*e*) M. W. Ghosn and C. Wolf, *J. Org. Chem.*, 2010, **75**, 6653; (*f*) J. M. Lenihan, M. J. Mailloux and A. B. Beeler, *Org. Process Res. Dev.*, 2022, **26**, 1812; (*g*) S. El-Arid, J. M. Lenihan, A. Jacobsen, A. B. Beeler and M. W. Grinstaff, *ACS Macro Lett.*, 2024, **13**, 607.

7 F. Medici, A. Puglisi, S. Rossi, L. Raimondi and M. Benaglia, *Org. Biomol. Chem.*, 2023, **21**, 2899.

8 (*a*) M. J. Genzink, M. D. Rossler, H. Recendiz and T. P. Yoon, *J. Am. Chem. Soc.*, 2023, **145**, 19182; (*b*) E. F. Plachinski, H. J. Kim, M. J. Genzink, K. M. Sanders, R. M. Kelch, I. A. Guzei and T. P. Yoon, *J. Am. Chem. Soc.*, 2024, **146**, 14948.

9 (*a*) K. Takagi, H. Fukaya, N. Miyake and Y. Sawaki, *Chem. Lett.*, 1988, 1053; (*b*) K. Takagi, T. Shichi, H. Usami and Y. Sawaki, *J. Am. Chem. Soc.*, 1993, **115**, 4339; (*c*) T. B. Nguyen and A. Al-Mourabit, *Photochem. Photobiol. Sci.*, 2016, **15**, 1115; (*d*) D. E. Marschner, C. O. Franck, D. Abt, H. Mutlu and C. Barner-Kowollik, *Chem. Commun.*, 2019, **55**, 9877; (*e*) J. Liu, Y. Shen, J. Peng, J. Sun and R. Lu, *J. Mater. Chem. C*, 2020, **8**, 3165; (*f*) T.-Y. Li, Y.-Z. Du, T.-Y. Xu, T.-L. Zhang and F. Tong, *Crystals*, 2024, **14**, 492.

10 (*a*) B. B. Yagci, Y. Zorlu and Y. E. Türkmen, *J. Org. Chem.*, 2021, **86**, 13118; (*b*) B. B. Yagci, B. Munir, Y. Zorlu and Y. E. Türkmen, *Synthesis*, 2023, **55**, 3777.

11 B. Munir, B. B. Yagci, Y. Zorlu and Y. E. Türkmen, *J. Org. Chem.*, 2024, **89**, 10409.

12 (*a*) A. Ichikawa, H. Ono and Y. Mikata, *Chem.–Asian J.*, 2012, **7**, 2294; (*b*) A. Ichikawa, H. Ono, T. Echigo and Y. Mikata, *CrystEngComm*, 2011, **13**, 4536.

13 (*a*) N. Harada, M. Watanabe, S. Kuwahara, A. Sugio, Y. Kasai and A. Ichikawa, *Tetrahedron: Asymmetry*, 2000, **11**, 1249; (*b*) N. Harada, *Chirality*, 2008, **20**, 691.

14 (*a*) A. N. Thadani, A. R. Stankovic and V. H. Rawal, *Proc. Natl. Acad. Sci. U. S. A.*, 2004, **101**, 5846; (*b*) Y. Huang, A. K. Unni, A. N. Thadani and V. H. Rawal, *Nature*, 2003, **424**, 146; (*c*) C. D. Anderson, T. Dudding, R. Gordillo and K. N. Houk, *Org. Lett.*, 2008, **10**, 2749.

15 S. M. Sartor, Y. M. Lattke, B. G. McCarthy, G. M. Miyake and N. M. Damrauer, *J. Phys. Chem. A*, 2019, **123**, 4727.

16 M. Nishio, *CrystEngComm*, 2004, **6**, 130.

17 (*a*) V. Enkelmann and G. Wegner, *J. Am. Chem. Soc.*, 1993, **115**, 10390; (*b*) T. Friščić and L. R. MacGillivray, *Z. Kristallogr.*, 2005, **220**, 351; (*c*) A. Chaudhary, A. Mohammad and S. M. Mobin, *Cryst. Growth Des.*, 2017, **17**, 2893.

18 Y. Gu, T. Kar and S. Scheiner, *J. Am. Chem. Soc.*, 1999, **121**, 9411.

19 (*a*) A. D. Becke, *J. Chem. Phys.*, 1993, **98**, 1372; (*b*) A. D. Becke, *J. Chem. Phys.*, 1993, **98**, 5648.

20 E. Caldeweyher, S. Ehlert, A. Hansen, H. Neugebauer, S. Spicher, C. Bannwarth and S. Grimme, *J. Chem. Phys.*, 2019, **150**, 154122.

21 F. Weigend and R. Ahlrichs, *Phys. Chem. Chem. Phys.*, 2005, **7**, 3297.

22 S. Kossmann and F. Neese, *J. Chem. Theory Comput.*, 2010, **6**, 2325.

23 F. Weigend, *Phys. Chem. Chem. Phys.*, 2006, **8**, 1057.

24 (*a*) S. Miertus, E. Scrocco and J. Tomasi, *Chem. Phys.*, 1981, **55**, 117; (*b*) M. Garcia-Ratés and F. Neese, *J. Comput. Chem.*, 2020, **41**, 922.

25 F. Neese, *Wiley Interdiscip. Rev.:Comput. Mol. Sci.*, 2022, e1606.

26 V. Asgeirsson, B. Orri Birgisson, R. Björnsson, U. Becker, F. Neese, C. Riplinger and H. Jonsson, *J. Chem. Theory Comput.*, 2021, **17**, 4929.

27 A.-R. Allouche, *J. Comput. Chem.*, 2011, **32**, 174.

28 C. F. Macrae, I. Sovago, S. J. Cottrell, P. T. A. Galek, P. McCabe, E. Pidcock, M. Platings, G. P. Shields, J. S. Stevens, M. Towler and P. A. Wood, *J. Appl. Crystallogr.*, 2020, **53**, 226.

29 T. Lei, C. Zhou, M.-Y. Huang, L.-M. Zhao, B. Yang, C. Ye, H. Xiao, Q.-Y. Meng, V. Ramamurthy, C.-H. Tung and L.-Z. Wu, *Angew. Chem., Int. Ed.*, 2017, **56**, 15407.

30 S. K. Pagire, A. Hossain, L. Traub, S. Kerres and O. Reiser, *Chem. Commun.*, 2017, **53**, 12072.

31 B. Dogga, C. S. A. Kumar and J. T. Joseph, *Eur. J. Org Chem.*, 2021, 309.

32 P. Daley-Dee, J. Clarke, S. Monfette and R. B. Bedford, *Org. Lett.*, 2025, **27**, 197.

33 A. M. Martínez, A. Puet, G. Domínguez, I. Alonso, R. Castro-Biondo and J. Pérez-Castells, *Org. Lett.*, 2023, **25**, 5923.

34 A. A. Upare, P. K. Gadekar, H. Sivaramakrishnan, N. Naik, V. M. Khedkar, D. Sarkar, A. Choudhari and S. M. Roopan, *Bioorg. Chem.*, 2019, **86**, 507.